PNAS
www.pnas.org

Supplementary Information for

**Self-assembled plasmonics for angle-independent structural color displays with actively addressed black states**

Daniel Franklin[1,2], Ziqian He[3], Pamela Mastranzo Ortega[2], Alireza Safaei[1,2], Pablo Cencillo-Abad[2], Shin-Tson Wu[3], Debashis Chanda[1, 2, 3*]

[1]Department of Physics, University of Central Florida, 4111 Libra Drive, Physical Sciences Bldg. 430, Orlando, Florida 32816, USA.

[2]NanoScience Technology Center, University of Central Florida, 12424 Research Parkway Suite 400, Orlando, Florida 32826, USA.

[3]CREOL, The College of Optics and Photonics, University of Central Florida, 4304 Scorpius St., Orlando, Florida 32816, USA.

[*]Correspondence and requests for materials should be addressed to D.C.
Email: Debashis.Chanda@ucf.edu

**This PDF file includes:**

Figures S1 to S10

**Other supplementary materials for this manuscript include the following:**

Movies S1



www.pnas.org/cgi/doi/10.1073/pnas.2001435117

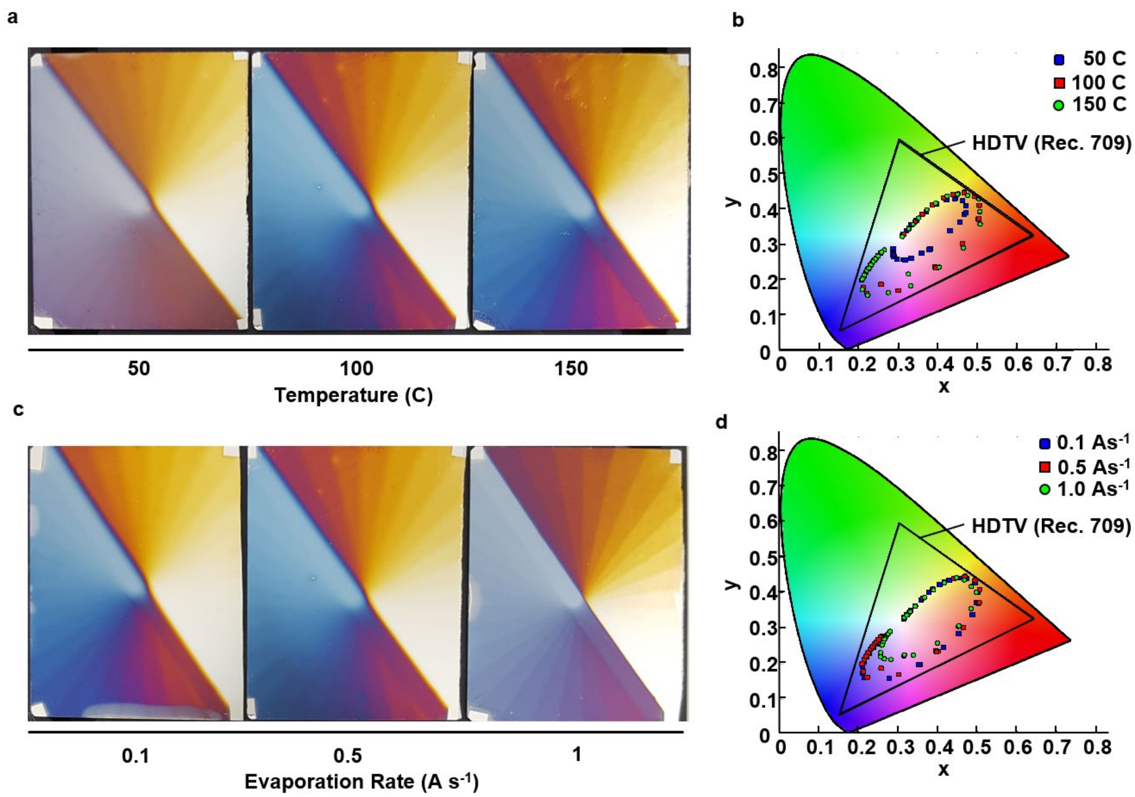


**Fig. S1 | Particle Formation Parameter Space and Impact on Color Quality. (a)** Camera images of 1 in x 2 in samples deposited at temperatures through 50 C to 150 C at a evaporation rate of 0.5 $As^{-1}$. **(b)** The 1931 CIE Chromaticity Diagram with color data obtained from the samples in (a). **(c)** Camera images of 1 in x 2 in samples deposited with evaporation rates form 0.1 $As^{-1}$ to 1 $As^{-1}$ at a temperature of 100 C. **(d)** The 1931 CIE Chromaticity Diagram with color data obtained from the samples in (c).

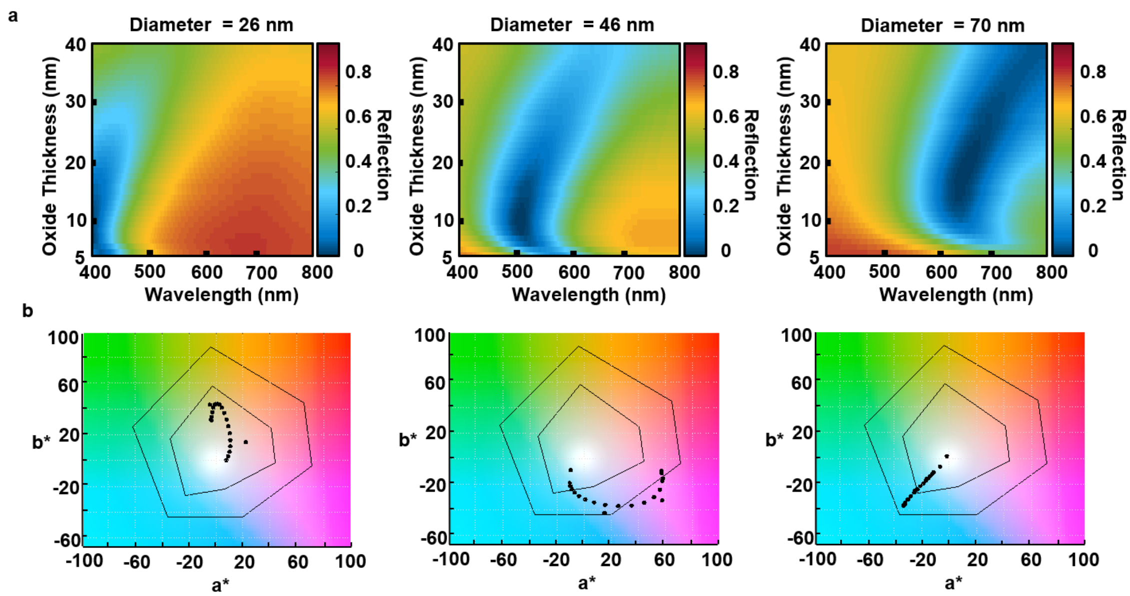


**Fig. S2 | Effect of Oxide Spacing Thickness. (a)** FDTD simulations of oblate aluminum ellipsoids separated from a mirror by an aluminum oxide spacing layer. Square boundary conditions are used which approximates the structure as a perfectly periodic array of singularly sized particles. As such, inhomogeneous line broadening due to particle size distributions is not accounted for. There is a distinct blue shift as oxide thickness increases from 5 nm to 10 nm, but then a red shift thereon. This is due to the inverse cube relationship in coupling strength between the particle film and mirror. **(b)** The impact of the oxide spacer thickness on surface color as represented on the CIE Lab color space. To provide context to this color quality, we overlay two color quality standards used in the commercial printing industry – ISO 12647-3 for the inner hexagon representing newsprint and SWOP Coated 1, ISO-standard on Grade 1 high quality photo paper for the outer hexagon.


**Fig. S3 | Polarization Photography of Plasmonic Surface**. Images of the plasmonic surface under unpolarized and linearly polarized states. Linear polarized images are obtained by inserting and rotating a linear polarizer (LPVISE100-A, Thorlabs) in front of a camera (Pixel 3XL, Google).

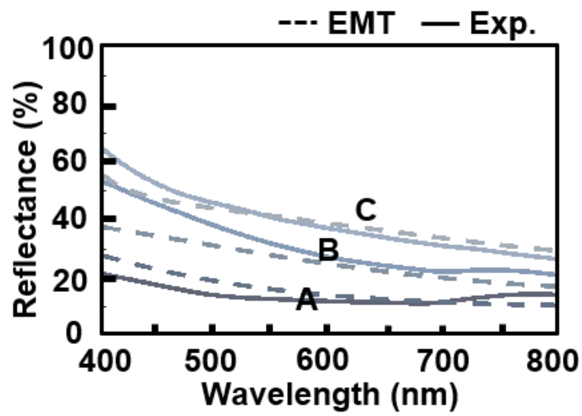


**Fig. S4 | Reflectance of Aluminum Nanoparticle Array.** Experimental and effective media theory spectra for a particle array on aluminum oxide but in absence of a mirror. A, B and C correspond to the particle dimensions defined in Figure 2. Results so a close agreement between experiment and theory. Line colors obtained from CIE Chromaticity functions.

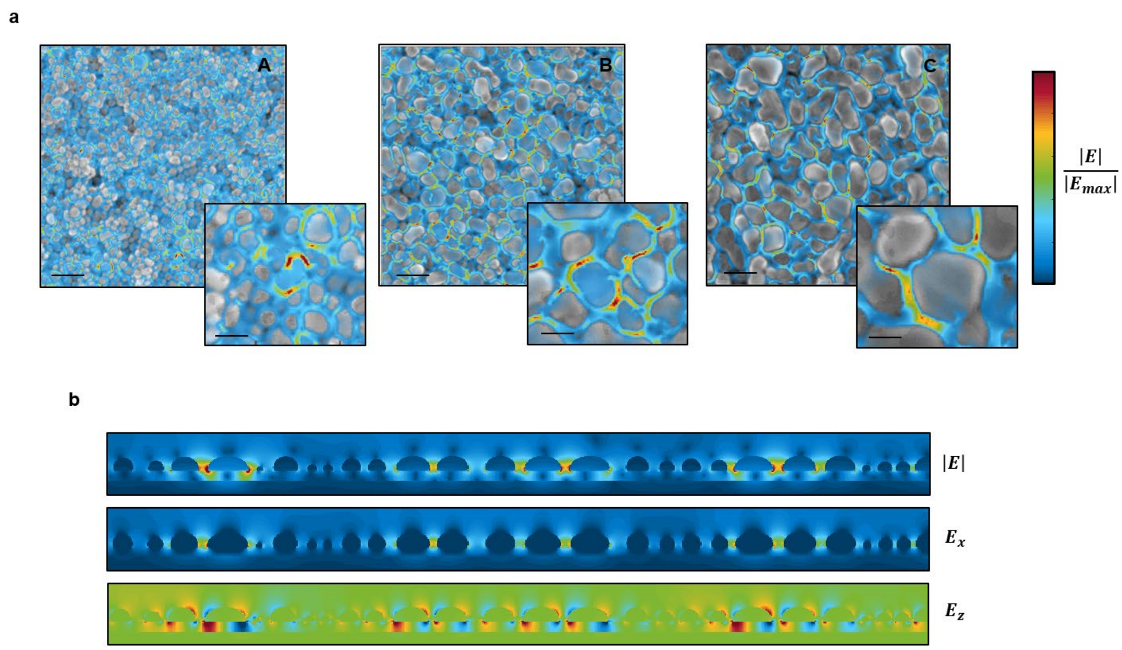


**Fig. S5 | FDTD Field Profiles (a)** Full volume FDTD simulations of imported SEM images. The same SEM images are overlaid on the resulting field profiles. **(b)** Various components of the electric field through a x-z slice of the surface showing strong localization of the field between particles and mirror.

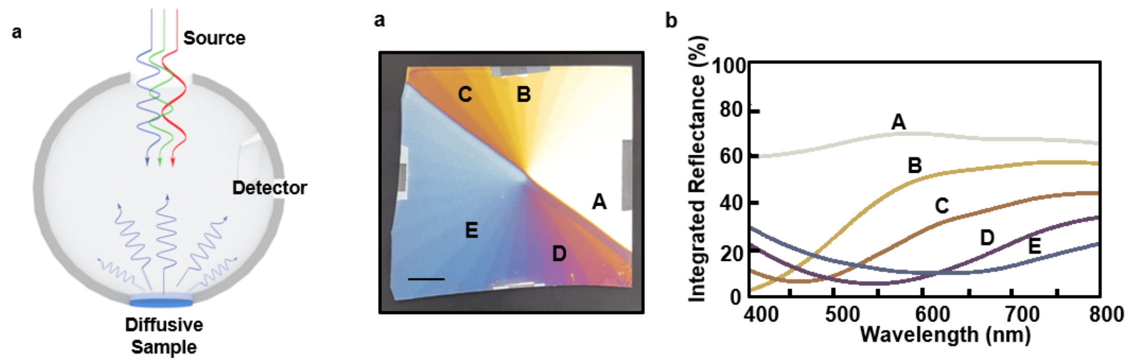


**Fig. S6 | Diffuse Reflectance. (a)** Illustration of the integrating sphere used to collect diffuse reflectance of the plasmonic surface when formed on sandblasted glass. **(b)** A camera image of the plasmonic system formed on a 2 in x 2 in piece of sandblasted glass which results in a near Lambertian diffuse reflectance. **(c)** Experimentally obtained integrated reflectance from the sample in (b) normalized to a diffuse Spectrareflect surface (LabSphere). Line colors are obtained through the CIE chromaticity matching functions. We see that much of the light is scattered but while maintaining the color of the underlying nanostructure. However, we also observe a slight broadening and weakening of the resonance. We attribute this to the extreme angles, more than 70°, at which a portion of particles are excited and to potential changes in particle distributions that may occur due to the evaporation on angled surfaces.

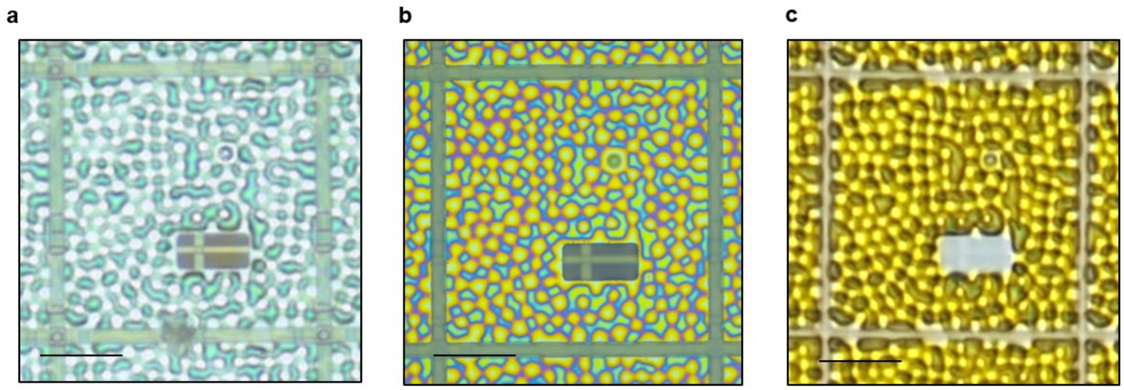


**Fig. S7 | Impact of Angle-Dependent Color on Commercial Reflective TFTs. (a)** Microscope image of a single pixel of the disassembled TFT after IPA rinsing away the original liquid crystal. **(b)** 5 nm of aluminum is evaporated on the surface in (a) which results in a color changing profile due to the thick polyimide alignment layer. This induces an angle dependent Fabry-Perot resonance which creates a change in color relating to the contours of the surface. **(c)** If instead, the surface in (a) is plasma etched to remove this polyimide layer, then ALD 10 nm aluminum oxide followed by 5 nm aluminum e-beam evaporated, the angle independent near field resonance can be obtained which results in vivid color over the uneven surface.

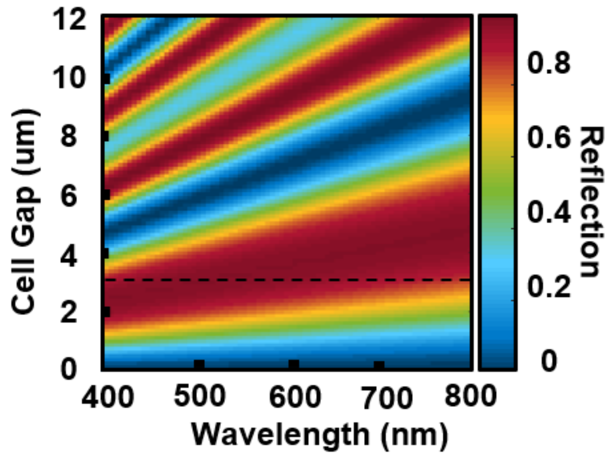


**Fig. S8 | Transfer Matrix Results of the 80º MTN LC Mode. (a)** The simulated reflectance for the bright-state (0V) of the MTN mode as a function of cell gap for a liquid crystal of $\Delta n = 0.07$. The dotted black line indicates the ideal cell gap thickness (3.5 μm) to achieve a maximum reflectance over the entire visible spectrum.

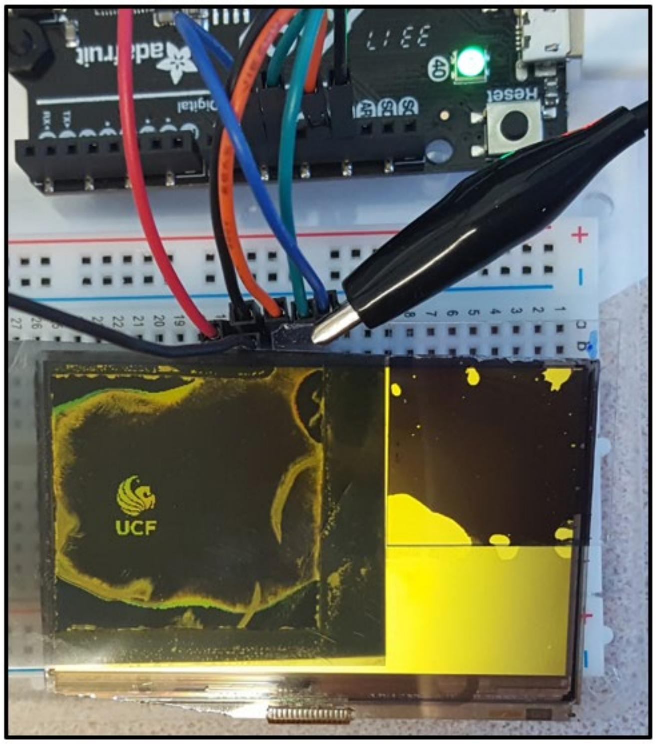


**Fig. S9 | Actively Addressed Hybrid LC-Plasmonic Display with Microcontroller Driver.** Camera image of whole display and connections to microcontroller. Left half of the display is the MTN LC mode, while the right half was experimentally used for dye-doped LC applications.

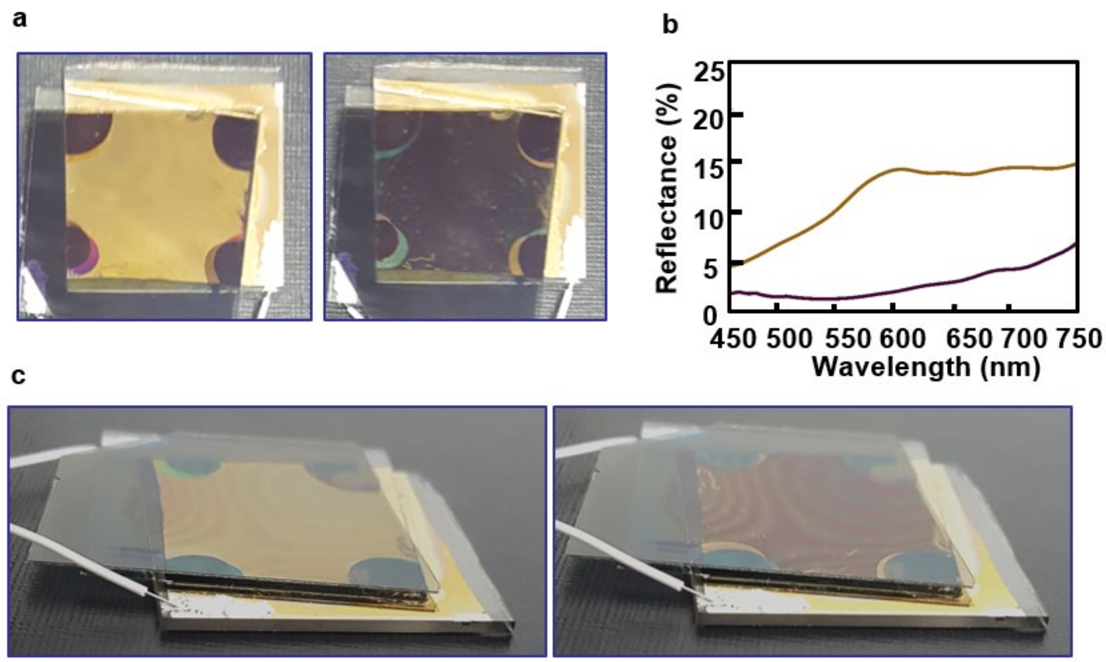


**Fig. S10 | Mixed Twisted Nematic Mode with Plasmonic Color. (a)** Single cell operation of an 80º mixed twisted nematic mode integrated with a 1 in x 1 in, yellow plasmonic substrate. The off-state results in the transmission of light through the cell while the on-state (in this case > 5 Vpp) blocks light at the second pass of the circular polarizer. **(b)** Reflection spectra of the sample in the two respective states, 0 Vpp and 5 Vpp. These results give a maximum contrast at 600 nm of 1/7.66. **(c)** The cell viewed at an incident angle of 50 degrees, showing minimal variation in color.